American Journal of Physics and Applications
2024, Vol. 12, No. 5, pp. 88-103
https://doi.org/10.11648/j.ajpa.20241205.11

Research Article

Studies About Atomic Compositions based on Synchrotron Radiation X- ray Microfluorescence (SR-μXRF) Analysis of Materials (at Micro- and Nano-Scale) Obtained by Sol-Gel Processes

Orlando Elguera Ysnaga*

Institute of Chemistry, Sao Carlos-University of Sao Paulo, Sao Paulo, Brazil

Abstract

Sol-gel is a wide-spread methodology for low-temperature synthesis of ceramics, nanocomposites and hybrid (inorganic-organic) materials. Ormosil (Organically Modified Silicates) belong to these class of hybrid materials, which have potential uses as optical materials, chemical sensors, catalysts, membranes, self-cleaning coatings. We are especially interested on the application of Synchrotron Radiation X-ray Microfluorescence (SR-μXRF) for the non-destructive analysis of such materials, benefiting of the high intensity obtained from this source of X-rays. SR-μXRF has demonstrated to be a useful analytical tool for qualitative and semi-quantitative determination of Hybrid films containing phosphotungstates ($[PW_{12}O_{40}]^{3-}$/PWA), in order to determine the local concentration, as also the correlation among elements. For ormosil films, SR-μXRF enabled the qualitative determination of Titanium (Ti) that is heterogeneously distributed, oppositely to the case of Zinc (Zn) and Tungsten (W). For PI-ORMOSIL-PWA films, SR-μXRF maps have shown the heterogeneous distribution of the Silicon (Si) and a quasi-homogenous distribution of Tungsten (W). SR-μXRF results for Silicon (Si) and Tungsten (W) are consistent with the corresponding concentrations obtained by ICP-OES analyses, which were taken as the reference results. For PDMSUr-PWA films, SR-μXRF mapping have shown the heterogenous distribution pattern for Tungsten (W) and the capacity for the identification of Bromine (Br). For these materials NAA analyses were taken as the reference results for Tungsten (W). Furthermore, they are presented the HorRat parameters, in order to estimate approximately the degree of heterogeneity of these materials, which are in agree with the observed in the corresponding mappings obtained by SR-μXRF, giving hints about segregation at surface and at bulk level. HorRat parameters for concentrations obtained by ICP-OES and NAA (bulk analyses) are close to the expected value ($_2$.0), which make possible using as reference values for SR-μXRF results (analyses at surface and medium-bulk levels), due to the non-existence of standards for these hybrid materials (at Micro- and Nano-Scale).

Keywords

SR-μXRF, ORMOSIL-TiO_2(Np)-PWA, ORMOSIL-Zn^{2+} Ions-PWA, PI- ORMOSIL-PWA, PDMSUr-PWA, HorRat

*Corresponding author: orlandoelguera@gmail.com (Orlando Elguera Ysnaga)

Received: 1 October 2024; **Accepted:** 5 November 2024; **Published:** 3 December 2024

1. Introduction

Organically modified silicates (Ormosil) are hybrid materials containing inorganic and organic structures that exhibit properties corresponding to ceramic and polymeric materials respectively. These hybrid characteristics enable the production of multifunctional materials. The structures of ormosil are based on a 3-D network of bonds constituted by Silicon and Oxygen -(Si-O-Si)- mainly[1], prepared more frequently by the Sol-Gel process[2]. Ormosil matrix constitutes a host for the occlusion of a diversity of chemical species (molecules, ions, clusters, etc.). Ormosil have applications as function of their optical, mechanical and chemical properties. Materials based on ormosil present among their advantages that can be built at low temperatures, and their structure and composition are tailored according to the applications required, for example membranes, coatings, contact lenses, laser components for optics, smart windows, nanocomposites, chemical sensors, catalysts, photochromic devices among others. However, ormosil present technical and scientific challenges. The knowledge of interactions between molecular and atomic constituents of ormosil is important, in order to understand their properties and applications [1-5].

We are especially interested in the nondestructive analysis of hybrid films (ORMOSIL- TiO_2(NPs)-PWA) based on the combination of ormosil chemical structure containing TiO_2 nanoparticles and phosphotungstates ($[PW_{12}O_{40}]^{3-}$/PWA). An unpublished work of our research group [6] has revealed from FTIR results the possible interaction of phosphotungstate with Titanium dioxide[3], based on intermolecular forces and/or ionic bonds. Gonçalves et al (2015) studied the effect of addition of TiO_2 nanoparticles (NPs) on the photochromic response of ormosil–PWA hybrid films. They demonstrated that small amounts of TiO_2 NPs can significantly improve the photochromic response and UV-sensitivity of Polyoxometalates (POMs)-based hybrid materials [7]. In order to explain the increase of their photochromic and photocatalytic properties of these ormosil with the content of TiO_2 NPs is necessary to know if the phosphotungstates and TiO_2 are sharing the same region or if there is proximity or no between them [8]. Due to the impossibility of identification of spatial distributions of Titanium within ormosil using FTIR, Raman and XRD, it was performed SEM-EDX. Nonetheless, it was not possible the identification of Titanium using this characterization technique, due to the low limit of detection of this element [6]. Thus, micro, semi-micro and trace-analysis could be suitable, in order to detect Titanium. One example of these analyses constitutes X-ray Micro-fluorescence (μXRF) that can be performed in solid state directly. For trace-level identification, the intensity of primary X-rays can be adjusted through of diverse mono-capillary and poly-capillary configurations that this analysis can present. Furthermore, if μXRF is assisted by Synchrotron radiation (SR-μXRF), limits of ppb can be achieved. Thus, SR-μXRF radiation can be suitable method of analysis for the determination of Titanium in ormosil films.

We also investigated samples of Hybrid photochromic films (ORMOSIL-Zn^{2+}ions-PWA) based on the combination of ormosil chemical structure containing Zn^{2+} and phosphotungstate ($[PW_{12}O_{40}]^{3-}$/PWA) ions, which have applications for UV-sensing devices and colorimetric dosimeters [9, 10]. SR-μXRF will enable the mapping of distribution of Zinc (Zn^{2+}ions) and Tungsten (phosphotungstates) in these films, in order to know if the phosphotungstates and Zn^{2+}ions share the same region [8, 10].

Furthermore, we investigated Hybrid films (PI-ORMOSIL-PWA) based on the combination of polyimide (PI), organically modified silicates (ORMOSIL) and phosphotungstates ($[PW_{12}O_{40}]^{3-}$/PWA), with potential application in hydrogen storage, membranes for fuel cells, insulating and anti-corrosive coatings. SR-μXRF will enable the mapping of distribution of Silicon (silicates) and Tungsten (phosphotungstates) in these films [8, 11, 12].

Finally, we investigated Hybrid films (PDMSUr-PWA) based on Polydimethylsiloxane (PDMS) and Urethanes (Ur) containing phosphotungstates ($[PW_{12}O_{40}]^{3-}$/PWA), with potential use in high-performance adhesives, elastomers, thermal and electrical insulators, coatings against corrosion, production of photochromic windows and fuel cell membranes. In order to better understand the photochromic, anti-corrosive, and mechanical properties of PDMSUr-PWA films, SR-μXRF will enable the knowledge about the distribution of Silicon (from silicates), Tungsten (from phosphotungstates) and Bromine (from Tetraethylammonium Bromide[4] or their derivatives species) in these films [8, 13-15].

μXRF is a useful microscopic tool in order to determine the spatial distribution of major, minor, and trace[5] elements in a sample. μXRF analysis is based on the localized excitation of a microscopic area on the surface of sample, being moved through of the micrometer- size beam in a raster movement, in order to perform single-point analysis, single-particle analysis, line scanning, elemental mapping and for 2-D XRF images. μXRF has underwent considerable progress, due mainly to the advances of Synchrotron Radiation (SR) facilities that including: X-ray sources, X-ray detectors and improved per-

1 Organic groups are linked through of -(Si-C)-bonds to the 3-D network of -(Si-O-Si)- bonds [1].

2 Sol–gel Chemistry consists in the colloidal synthesis of Sol (diameters of 1–100 nm) and Gel (sub-micrometer dimensions) [5]

3 Controlling the interaction between phosphotungstate and TiO_2 nanoparticles, as well as the edge energy of the semiconductor conduction band, one can design systems that will be the most efficient photocatalytic photochromic materials. Photocatalysis is produced by the gap in the radiated TiO_2 valence band, and benefited by the electron transfer from the TiO_2 conduction band to the phosphotungstate [6].

4 TEAB (Tetraethylammonium Bromide) was the catalyst in the synthesis of bis (cyclic carbonate) poly(dimethylsiloxane) (CCPDMS), one previous step for synthesis of PDMSUr-PWA [14].

5 It is one of the important applications of Synchrotron X-ray microbeams [22].

formance of X-ray optics (lenses, focusing instrumentation), which opening new application fields for XRF analysis. Among these fields of applications are mentioned: biology, chemistry, geology, industrial, environmental, archaeology, agriculture, etc. At Synchrotron Radiation X-ray fluorescence (SR-μXRF), the brilliance[6] achieved by this radiation and the incident flux on the sample is directly responsible for the enhancement of XRF sensitivity[7], improving the quality of characterization of materials [16-18]. μXRF is a nondestructive method, requires little sample preparation and present feasibility for quantitative analysis, allowing simultaneous multielement detection [19-21]. Among the merits of SR-μXRF are that the rays produced have intensities 10^4-10^5 times higher than the corresponding to the μXRF laboratory spectrometers, presenting detection limits (LOD) [8] in the range of 10^{-12}-10^{-14} g [24] [9], with a resolution of about of tens of micrometers [16, 25]. Detection Limits are improved in SR-μXRF by X-ray focusing optics that reduce the background intensity in the X-ray spectrum [16]. Comparing with other X-ray methods SR-μXRF presents a penetration depth[10] between the obtained from EPXMA (Electron Probe X-ray Microanalysis) and PIXE (Proton Induced X-ray Emission). For the element Pb (Z=82) e.g., the penetration depth of EPXMA, μXRF and PIXE are 2.0, 10 and 37 μm respectively [24][11].

Since these hybrid materials constitute complex matrices to analyze, the development of methods for quantification and mapping of their element's constituents are crucial for their applicability. The dimensions of μXRF beam enable the analysis of heterogenous samples [12]. One of the most valuable features of the μXRF is the semi-quantitative determination by the method of Fundamental Parameters (FP) [13], which includes physical, geometrical and technical parameters, in order to estimate the concentration of chemical elements [26]. This method is very useful in the case of lack of certified reference materials for heterogeneous and complex matrices, as is in our case.

The heterogeneity of the distribution of dopants in the ormosil films can affect their photochromic (at bulk level) and photocatalytic (at surface level) properties. One way to semi-quantify the heterogeneity could be by means of Horwitz Ratio (HorRat):

$$HorRat = \frac{\mathrm{RSD}_R}{\mathrm{PRSD}_R} \quad (1)$$

Where RSD_R is the relative standard deviation from actual performance data. RSD_R could be substituted by the Coefficient of Variation (% Coefficient of Variation= 100*(Standard Deviation)/ (Mean Concentration value), in order to obtain an approximation to the HorRat parameter [27, 28]. PRSD_R is the predicted relative standard deviation calculated from Horwitz equation:

$$PRSDR = 2^{(1-0.5\log C)} \quad (2)$$

Where C is Concentration expressed in mass fraction, The accepted values for HorRat parameter are between 0.5 and 2.

For this reason, the present study proposes an analytical methodology for these hybrid films based on the comparison of elemental composition obtained from the combination of different, independent, well-established and recognized methods of analysis as: Inductively Coupled Plasma Optical Emission Spectrometry (ICP-OES) and Neutron Activation Analysis (NAA), in order to obtain one reference value. The HorRat parameter is applied in order to intend validate this methodology. Thus, it is possible using SR- μXRF, in order to get an approximation for quantification for these hybrid nanomaterials.

2. Materials and Methods

2.1. Materials

2.1.1. Samples and Reference Materials Condition

1. Samples Analyzed:

1. Hybrid films (ORMOSIL-TiO_2(NPs)-PWA) deposited by Drop-coating on Ultra-thin Mylar® (from Sietronics Pty Ltd Company) substrates of thickness 3.6 μm. Code of samples: A7, A8 [6].
2. Hybrid photochromic films (ORMOSIL-Zn^{2+}ions-PWA) deposited by Drop-coating on Ultra-thin Mylar® (from Sietronics Pty Ltd Company) substrates of thickness 3.6 μm. Code of samples: ZE1, ZE0.5 [9, 10].
3. Hybrid films (PI-ORMOSIL-PWA). Code of samples: PATH-1, PATH-2, PATH-3 [11, 12].
4. Hybrid films (PDMSUr-PWA). Code of samples: PUK-32, PUK-30, PUK-42 [8, 13].

2. Reference Materials:

1. SR-μXRF: the reference materials used for measurements were standards of Zinc Telluride (ZnTe), with density=46.1 μg/cm^2 (±5%), and Gold (Au), with density=47.2 μg/cm^2 (±5%), provided by the Micromatter Company, under the form of thin films on Mylar® substrate.
2. ICP-OES: the certified reference materials used for the

6 Defined as (photon flux)/(unit source area x unit solid angle x unit energy): (ps-1.eV^{-1}.mm^{-1}.mrad^{-1}) [23].

7 Synchrotron sources can be 8-12 orders of magnitude more brilliant than the conventional X-ray sources [23].

8 LOD depends on the XRF yield, energy of the analyzed element, intensity of the primary X-rays, matrix composition, the focusing optics and atomic number (Z) of the analyzed element [16].

9 Janssens, K. (1996). Synchrotron Radiation Induced X-ray Microfluorescence Analysis. Mikrochim. Acta [Suppl.] 13, p. 87-115 [24].

10 The depth of analysis depends on the XRF energy and matrix composition.

11 Drop in the depth of penetration of X-ray methods with the particles/photons with the charge is determined by the gradual loss of energy that occurs as a result of inelastic scattering, the product of interactions with matter.

12 In conventional XRF, the analysis area on the sample is typically 10 mm in diameter.

13 Fundamental Parameters (FP) that take in consideration the experimental set-up (geometrical parameters); the absorption coefficient, the absorption jump ratio, and the fluorescent yield of XRF line (physical parameters), in order to approximate to the experimental conditions of the measurements without need to make an analytical curve [29].

measurements were standard solutions for AAS of 1000 mg/Kg TraceCERT® for Silicon, Titanium and Tungsten.

3. NAA: the certified reference material used for the measurements was a foil of Tungsten Goodfellow Brandt of high-purity (99.95%), with 6 μm of thickness.

2.1.2. Samples Preparation

(i). Hybrid Films Containing Phosphotungstates Doped with TiO_2 Nanoparticles (ORMOSIL-TiO_2 (NPs)-PWA)

The detailed synthesis of these ormosil films doped with TiO_2 nanoparticles, based on the Sol–Gel method, are described on the references [6, 7]. The Sol formulations used for the preparation of ormosil films are reported in Table 1; all solutions were prepared in polypropylene beakers. The procedure for preparation of these hybrid films is as follow: the alkoxysilanes TEOS ($Si(OC_2H_5)4$), GLYMO ($C_{10}H_{21}NO_3Si$) and BUTS ($C_9H_{20}O_5Si$) were add to the beakers with a micropipette, and then add 25 mL of solvent mixture (ethanol/acetone 9:1) under magnetic stirring; immediately afterwards 25 mL of freshly prepared PWA solution in the mixture ethanol/acetone, which was added under magnetic stirring for 30 min. The last step consisted in adding Titanium Dioxide (TiO_2) nanoparticles in suspension (0.1%m/v) with different concentrations with a micropipette. The mixture was left under magnetic stirring for 10 min before to be deposited on substrates. The films were deposited by Drop-coating on static Mylar® substrates and dried under ambient atmosphere. The details of the formulation used during preparation by Sol-Gel processes for samples to be analyzed by SR-μXRF are summarized in Table 1:

Table 1. *Formulations used in the preparation of Hybrid films (ORMOSIL-TiO_2(NPs)-PWA) during preparation by Sol-Gel method [6].*

Sample	TEOS	GLYMO	BUTS	PWA	Volume (10^{-6} L)	Nominal
Code	10^{-3} mol	10^{-3} mol	10^{-3} mol	10^{-3} mol	TiO_2 nanoparticles suspension 0.1%.	Titanium, Concentration [Ti] (% wt/wt)
A7	9	6.8	1.5	0.75	$1.0.10^3$	0.83
A8	9	6.8	1.5	0.75	$2.0.10^3$	1.63

Sources: I) Table 1 (except the column corresponding to [Ti] nominal concentration): [6, 7]. For the column corresponding to [Ti] concentration): [8] from Sol-Gel reactions, considering the absence of solvent.

(ii). Hybrid Photochromic Films Containing Phosphotungstates Doped with Zn^{2+}ions (ORMOSIL-Zn^{2+}ions-PWA)

The synthesis of ormosil films doped with Zn^{2+} ions, based on the Sol–Gel method, are described on [9, 10]. The sol formulations of the prepared samples are summarized in Table 2. The procedure for preparation of these hybrid films is as follow: the alkoxysilanes TEOS, GLYMO and BUTS were dissolved in 25 mL of ethanol in a polypropylene beaker, followed by addition of 25 mL of freshly prepared PWA solution in ethanol under stirring. Then, ZnO suspension (0. 1 mol. L^{-1}) in ethanol was added and the mixture was kept under magnetic stirring for 5 minutes to homogenize the sol. Finally, 825 μL of deionized water was added to this mixture and kept under stirring for more 10 minutes before to be deposited on substrates. The films were deposited by Drop-coating on static Mylar® substrates and dried under ambient atmosphere. The details of the formulations used during preparation by Sol-Gel processes for samples to be analyzed by SR-μXRF are summarized in Table 2:

Table 2. *Formulations used in the preparation of Hybrid films (ORMOSIL-Zn^{2+}ions-PWA) during preparation by Sol-Gel method [10].*

Sample	TEOS	GLYMO	BUTS	PWA	$Zn(NO_3)_2$	Nominal Zinc
Code	10^{-3} mol	10^{-3} mol	10^{-3} mol	10^{-3} mol	10^{-3} mol	Concentration [Zn] (% wt/wt)
Zn 0.5	9	6.8	1.5	0.75	0.1	0.19
Zn 1.0	9	6.8	1.5	0.75	0.2	0.38

Sources: I) Table 2(except the column corresponding to [Zn] nominal concentration): [10]; II) Table 2 (For the column corresponding to [Zn] concentration): [8] from Sol-Gel reactions, considering the absence of solvent.

(iii). Hybrid Films of Polyimide (PI) and Ormosil Containing Phosphotungstates (PI-ORMOSIL-PWA)

The formulations and synthesis of PI- ORMOSIL-PWA films are described in [11, 12]. The details of the samples analyzed by SR-μXRF are summarized in Table 3.

Table 3. *Details of Hybrid films PI-ORMOSIL-PWA.*

Sample Code	TEOS 10^{-3} mol	APTES 10^{-3} mol	PWA 10^{-5} mol	[Si] (%wt/wt)	[W] (%wt/wt)
PATH-1	0.38	0.09	0.31	1.47	8.16
PATH-2	1.51	0.36	0.31	4.59	7.03
PATH-3	2.27	0.53	0.31	6.77	6.27

Sources: I) Table 3 (except the columns corresponding to [Si] and [W] concentrations): [8]-page 306/II) Table 3 (For the columns corresponding to [Si] and [W] concentrations): [8]-pages 306, 380. These results are obtained considering the absence of solvent.

(iv). Hybrid Films Based on Polydimethylsiloxane (PDMS) and Urethanes (Ur) Containing Phosphotungstates (PDMSUr-PWA)

The formulations and synthesis of PDMSUr-PWA films are described in [14, 15]; so, as their Tungsten nominal atomic compositions are described in [8]. The details of the samples analyzed by SR-μXRF are summarized in Table 4.

Table 4. *Details of Hybrid films PDMSUr-PWA.*

Sample Code	[W]* (% wt/wt)
PUK32	24.7
PUK30	35.0
PUK42	41.8

Source: [8]. (*) Relative to the total mass of PDMSUr precursors (CCPDMS+APTES) without solvent.

2.2. Methods of Analysis

2.2.1. SR-μXRF Instrumentation and Operational Conditions for Experiments

X-ray Micro-fluorescence (SR-μXRF) experiments were performed at D09B-XRF line of LNLS synchrotron radiation facility (Campinas-Brazil). The experiments were done in atmospheric pressure. The configuration of setup chosen for SR-μXRF experiments [30] includes:

1. Source (storage ring) of 1.4 GeV provides a polychromatic X-ray beam, in which photon flux ranging from $3.9x10^{10}$ to $2.31x10^{11}$ photons/s and an energy tuned at the range of 4–16 keV.
2. Micro-focusing system, which is based on: a rotation/translation sample stage that contains three motors (x, y, z direction) driven by stepping motors (the sample is scanned in step-by-step displacements during scans of images), in order to focalize;
3. Sample chamber, which can be evacuated, in order to avoid the attenuation of fluorescent X-ray and to suppress the scattered radiation by the air;
4. Two elliptic non-plane Kirkpatrick-Baez (KB) mirrors in order to focus X-ray beams, reflecting them on their coated surface mirrors (with reduced aberration);
5. Microscope in order to identify the portion of sample to be analyzed;
6. Energy X-ray Dispersive Si (Li) solid-state transmission detector (Si (Li)-SSD) with 165 eV FWHM at 5.9 keV that additionally contain 6 sets of array foils (each array consists of 8 foils of pure Aluminum, each one 15 μm of thickness). The semiconductor detector is cooled by N_2 (l) in order to overcome the heat load.
7. The elliptic microbeam obtained had the following dimensions in the micrometers range: 18 μm (major-axis) x 9 μm (minor-axis), allowing the focusing on sample position. The working distance was about 0.1 m [30].

The number of sampling points (each point depicts to one XRF spectrum) collected for SR-μXRF maps were:

1. Hybrid ORMOSIL-TiO_2(NPs)-PWA films: $_{22}$0 points for Titanium and Tungsten
2. Hybrid ORMOSIL-Zn^{2+}ions-PWA films: 400 points for Zinc and Tungsten
3. Hybrid PI-ORMOSIL-PWA films: 400 points for Silicon and Tungsten
4. Hybrid PDMSUr-PWA films: 420 points for Silicon, Bromine and Tungsten

SR-μXRF mappings (scanned at zig-zag mode) was carried out on a surface area of 1 cm^2. The time of acquisition of SR-μXRF analysis by point was 5 seconds. The raw spectral data were analyzed using the Readcnfmca v2.0 program (developed at the LNLS XRF Beamline) and PyMCA

(http://pymca.sourceforge.net/documentation.html [31]) X-ray Fluorescence version 4.4 program (developed by the Software Group of the European Synchrotron Radiation Facility-ESRF) [31, 32], in order to extract the XRF intensities for each point measured, for the posterior processing of elemental maps. The pixel size of the SR-μXRF maps was 26 μm [8]. In order to perform semi-quantitative determination, in addition to the PyMCA 4.4 version was used the WinAxil also [33, 34] program version 2.0, both of them based on the Fundamental Parameter Method (FP). For FP was used the correspondent parameters of the D09B-XRF line of LNLS-Campinas-Brazil [29]. The XRF excitation energies chosen were for Silicon (Si-Kα: 1.740 keV), Titanium (Ti-Kα: 4.512), Tungsten (W-Lα: 8.398 keV) and Zinc (Zn-Kα: 8.637 keV) and Bromine (Br-Kα: 11.924 KeV). Figures 1 and 2 show the experimental setup and applications for SR- μXRF measurements:

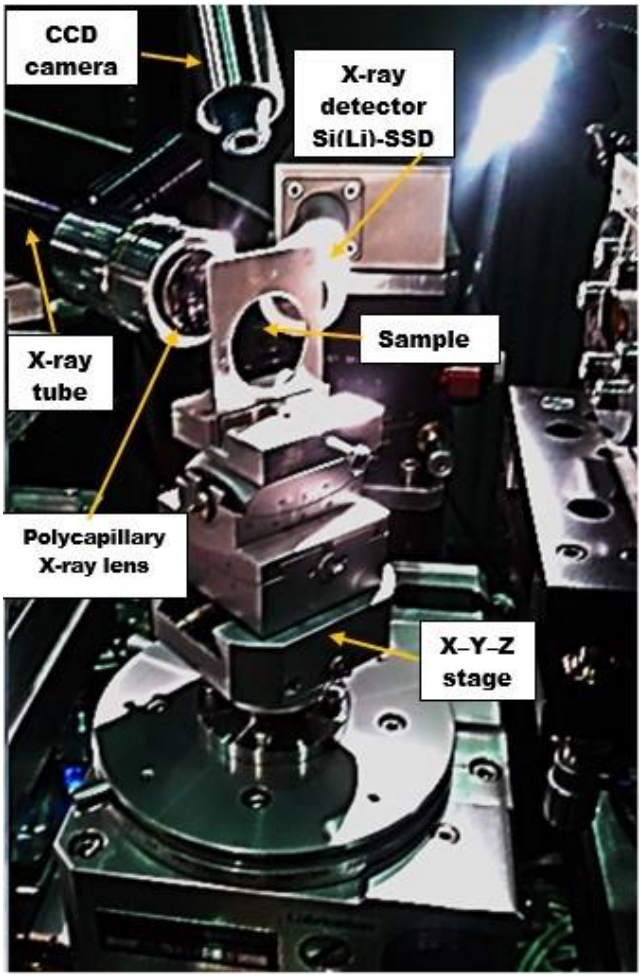

Figure 1. *Experimental setup for SR-μXRF measurements at LNLS.*

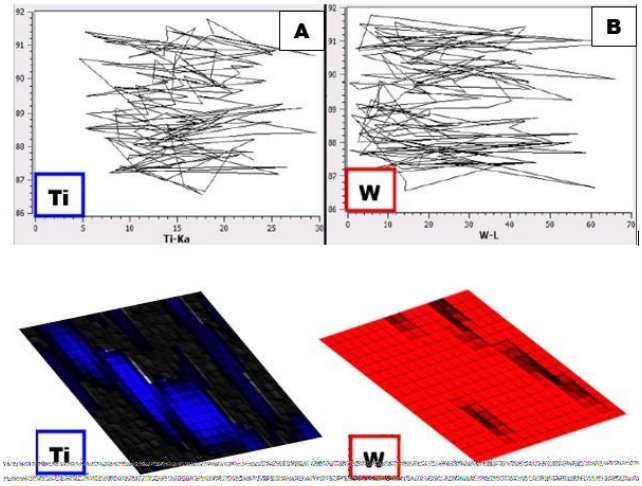

Figure 2. *SR-μXRF line scanning and 2-D elemental mapping of Titanium (Ti) and Tungsten (W) respectively.*

2.2.2. Inductively Coupled Optical Emission Spectroscopy (ICP-OES)

1. Method of Digestion for ICP-OES Analysis of Hybrid films PI-ORMOSIL-PWA

For ICP-OES analysis, the samples under film form (0.1 g) were poured in Polytetrafluorethylene (PTFE) vessels, in which were added the mixture 2 ml HNO3 (65% m/m)/1.0 ml HClO4 (70% m/m) and heated at 180 ℃ until total dryness (in order to destroy the organic matter). Subsequently, retire the PTFE vessels at ambient temperature for 1 hour approximately. In the sequence, at T=20 ℃ were added $_2$ ml HF (48 w/w%) to the PTFE vessels until total dissolution, and after 0.5 ml HNO3 (65% w/w%) was added to the digested sample. Posteriorly, the solution acidified was carefully transferred to the 25 ml volumetric plastic flasks, and in the sequence deionized water (Milli-Q water) was added, in order to complete this volume. Finally, these volumetric plastic flasks were vigorously agitated previous to the ICP-OES analysis. The reagents used were of analytical grade (Merck or similar) [8].

2. Instrumentation for ICP-OES Analysis

ICP-OES analysis for Silicon (Si) and Tungsten (W) contained in the PI-ORMOSIL- PWA films were performed by the Perkin Elmer Optima 3000 DV ICP AES in the sequential mode performed at the Analytical Center of the Instituto de Qu ímica de S ão Carlos- Universidade de S ão Paulo (IQSC-USP). The emission wavelengths chosen for Silicon, Titanium and Tungsten were $_2$88.158 nm, 334, 903 nm and $_{22}$4.876 nm respectively, being the configuration of the plasma torch in the axial mode (number of measurements per sample=3) [8].

2.2.3. Instrumental Neutron Activation Analysis (NAA)

NAA analysis for PDMSUr-PWA samples were irradiated in the IEA-R1 nuclear reactor at IPEN-CNEN/SP (IEA-R1, 3–4.5 MW, pool type) with a thermal neutron flux 1.76.1012 neutrons $cm^{-2}.s^{-1}$, time range per channel 300-900 s, in order to determinate Tungsten. The IEA-R1 nuclear reactor has Uranium enriched to 20% in the isotope 235U as fuel and light water as moderator, operating at power of 4.5 MW. The nuclear reaction of neutron activation for Tungsten nucleus is 186 W (n, γ) 187 W. For W187 isotope (T1/2 = 24 h; Eɣ = 479, 481, 552, 618, 687, 745, 772 keV), an irradiation time of 30 s followed by a decay time of 2 h were used. The gamma spectrometer system used consisted on a high purity Germanium (HPGe) semiconductor detector with high resolution (FWHM = 1.87 keV at 1332 keV of 60Co), which was coupled to an ADCAM-ORTEC 919E MCA analyzer and a micro-PC, in order to measure the induced gamma-ray activities. The source to sample distance was 12.5 cm. The gamma spectral analyses evaluations were performed using the IDF computer code [8, 35].

3. Results and Discussions

3.1. SR-µXRF 2-D Mapping

3.1.1. SR-µXRF Mapping of Hybrid ORMOSIL-TiO_2 (NPs)-PWA Films

Figure 3A-3C show the SR-µXRF mapping of Titanium (Ti-Kα), Tungsten (W-Lα) and their respective correlation spatial mappings for ORMOSIL-TiO_2(NPs)-PWA films [8]:

Figure 3A shows the accomplishment of SR-µXRF in the identification of Titanium (Ti), which is heterogeneously distributed, in the Hybrid ORMOSIL-TiO_2 (NPs)-PWA films. Titanium could not be confirmed by the EDS microanalysis due to its low concentration [7]. The typical detection limit of µXRF for Titanium is 100 mg. Kg^{-1} [16]. Figure 3B shows the sample A8 presents more homogeneous distribution pattern (fewer black regions) of Tungsten than the sample A7 [8]. Similar trend of homogeneity for Tungsten (W) was shown in EDX mapping for ORMOSIL-TiO_2(NPs)-PWA films [6]. Titanium+Tungsten regions support the Raman/IR results about the possible electrostatic/intermolecular interaction of polyoxometalate ($[PW_{12}O_{40}]^{3-}$) with TiO_2 nanoparticles [6, 7]. TiO_2+$[PW_{12}O_{40}]^{3-}$ could constitute a colloidal system [8]. FTIR and Raman spectroscopy demonstrated the entrapment of PWA in hybrid organosilicate network [7]. Furthermore, the sample A8, with the highest TiO_2 nanoparticle content (see Table 1), exhibits higher counts rate for Tungsten (400000) than the sample A7 (160000). Figure 3C shows that the sample A8 exhibits more common regions (pink color) of Titanium+Tungsten than the sample A7 [8]. From these observations, it can be inferred that there is direct relationship between the Titanium and Tungsten intensities.

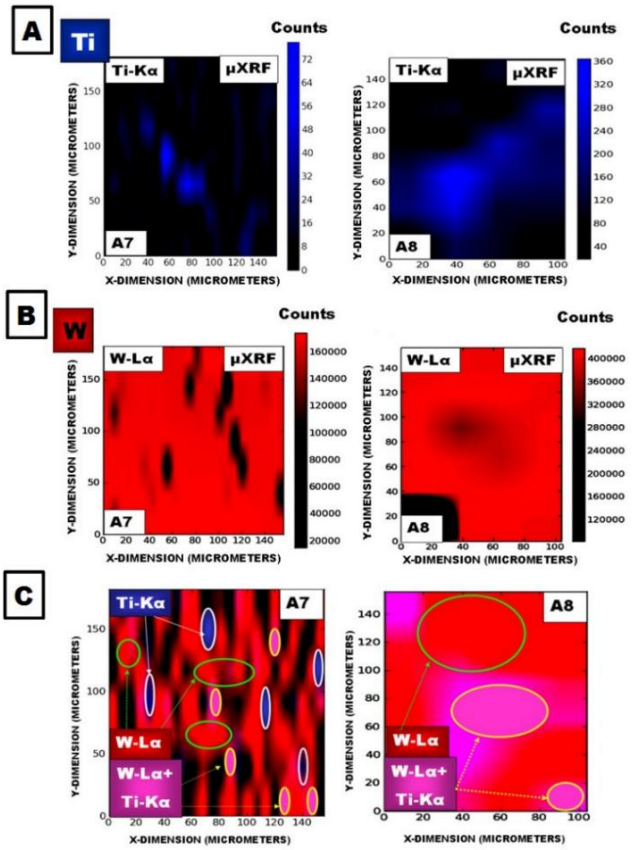

Figure 3. *SR-µXRF mappings of Hybrid ORMOSIL-TiO_2(NPs)-PWA films: Upper: 3A) Titanium A7 (left) and A8 (right); Center: 3B Tungsten A7 (left) and A8 (right); Lower: 3C) SR-µXRF correlation spatial mapping (Titanium: blue, Tungsten: red, Titanium+ Tungsten: pink) for films A7 (left) and A8 (right).*

3.1.2. SR-µXRF Mapping of Hybrid ORMOSIL-Zn^{2+}ions-PWA Films

Figure 4A-4C show the SR-µXRF mapping of Zinc (Zn-Kα) and Tungsten (W-Lα) and their correlation spatial mapping for ORMOSIL-Zn^{2+}ions-PWA films [8]:

Figure 4A-4C show the homogeneity of the distribution of Zinc (Zn) and Tungsten (W) in the Hybrid ORMOSIL-Zn^{2+} ions-PWA films deposited on Mylar® substrates. In the correlation spatial mapping (Figure 8), Zinc and Tungsten present similar distribution patterns (few regions isolated corresponding to these elements). Zn^{2+} ions were found in the ormosil films due that ZnO nanoparticles were completely dissolved due to the presence of phosphotungstic acid ($H_3PW_{12}O_{40}$). This was confirmed by UV-Vis absorption spectroscopy and Raman spectroscopy [9]. These similar distribution patterns of Zn and W are supported by STEM images and EDX spectra that revealed aggregates of compounds (of ionic nature) containing Zinc and Tungsten in

these hybrid films, such as is described in [10]. XANES (X-ray Absorption Near Edge Structure) spectra of the Zn K-edge for different compounds could give support about the possible formation of the salt compound $[Zn(OH_2)_6]_{x/2}H_{3-x}PW_{12}O_{40}$. Raman Spectroscopy confirmed that the Keggin structure of PWA is preserved, after being entrapped in the Ormosil matrix by Sol-Gel process [10].

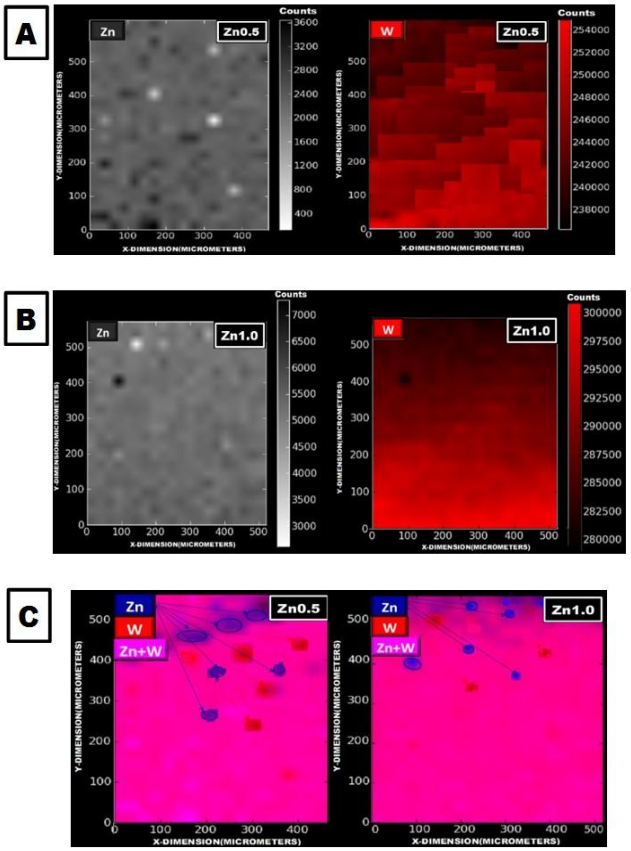

Figure 4. SR-μXRF mapping of Hybrid ORMOSIL-Zn^{2+}ions-PWA films: Upper: 4A) Zn 0.5 sample: Zinc (left) and Tungsten (right); Center: 4B) Zn 1.0 sample: Zinc (left) and Tungsten (right); Lower: 4C) SR-μXRF correlation spatial mapping (Zinc-blue, Tungsten-red, Zinc +Tungsten (pink)) for samples Zn 0.5 (right) and Zn 1.0 (left).

3.1.3. SR-μXRF Mapping of Hybrid PI-ORMOSIL-PWA Films

Figure 5A-5C show the SR-μXRF correlation mapping of Silicon (Si-K_α line) and Tungsten (W-L_α line) for PI-ORMOSIL-PWA films on both faces (front and back sides) [8]:

SR-μXRF mappings of PI-ORMOSIL-PWA films illustrated in Figure 5A-5C show different distribution patterns of Silicon (green color) that depend on the side of the film analyzed (front and back) [8]. From this fact, we could infer segregation of Silicon through the thickness for these materials. This observation is supported by the XRD characterization showed in [11] establishing that the surface of these films presents a different structural organization than their volume. Furthermore, the front sides of PATH- 1 and PATH-3 films exhibit common regions of Silicon+Tungsten (yellow) that could indicate some type of interaction between these elements (possible ionic compound formed: $\equiv(Si–OH_2)^+(H_2PW_{12}O_{40})^-$, $[\equiv Si–(CH_2)_3–NH_3]^+(H_2PW1_2O_{40})^-$[18]). The coverture of Silicon+Tungsten regions (yellow) is major for PATH-3 than for PATH-1, corroborated the analysis of SEM characterizations of PI-ORMOSIL-PWA films. This analysis show that the PATH-3 sample exhibits greater sizes (900 ±300 nm) and a major number of aggregates than PATH-1 sample (267 ±52 nm) [8]. These results are in agree with the [11] that revealed from T-FTNIR (Near Fourier Transform Infrared in Transmission mode Spectroscopy) and NMR and XANES experiments that the structure of PWA does not undergo important changes in its structure.

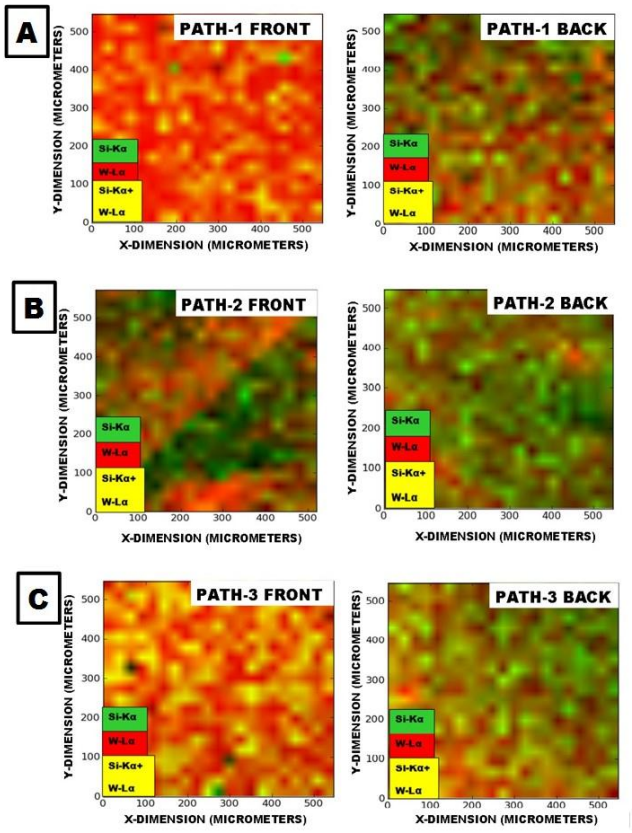

Figure 5. SR-μXRF Correlation Spatial Mappings (Silicon +Tungsten) Hybrid PI-ORMOSIL-PWA films: Upper: 5A) PATH-1: front (left), back (right); Center: 5B) PATH-2: front (left), back (right); Lower: 5C) PATH-3: front (left), back (right). Legend: Silicon (Si-K_α, green), Tungsten (W-L_α, red), and Silicon +Tungsten (yellow).

3.1.4. SR-μXRF Mapping of Hybrid PDMSUr-PWA Films

Figure 6A and 6B show the SR-μXRF correlation mapping of Silicon (Si-Kα line), Tungsten (W-Lα line) and Bromine

(Br- Kα line) for PDMSUr-PWA films:

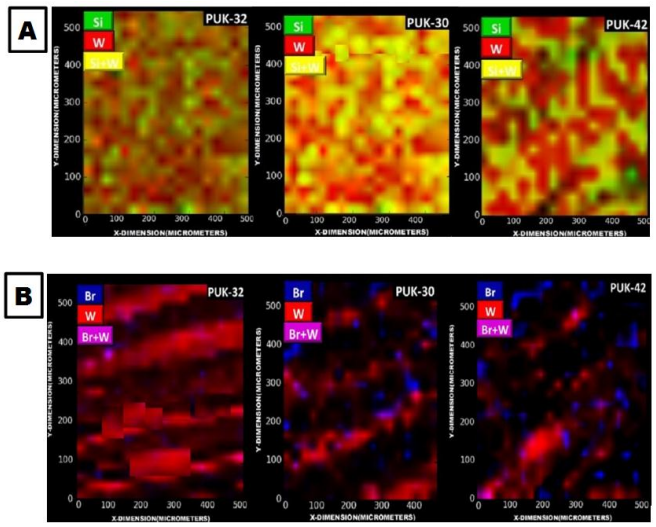

Figure 6*. SR-μXRF correlation spatial mappings. Upper: 6A). SR-μXRF correlation spatial mapping (Silicon and Tungsten) for samples PUK32 (left), PUK30 (center) and PUK42 (right). Lower: 6B). SR-μXRF correlation spatial mapping (Bromine and Tungsten) for samples PUK32 (left), PUK30 (center) and PUK42 (right). Legend: Bromine (Br-Kα, blue), Tungsten (W-Lα, red), and Bromine + Tungsten (violet).*

SR-μXRF mappings in Figure 6A have shown a direct dependence between the concentration of PWA and the coverture of Tungsten (red regions) and Silicon+Tungsten (yellow color) at surface level in these materials [8]. From this observation, we could infer an interaction between these elements. Figure 6B exhibits the irregular distribution of Bromine and regions scarce common with the Tungsten at the SR-μXRF of Br+W maps. FTIR experiments showed that PWA keeps its structure almost unchanged inside of these hybrid films by means of interactions with the organic/inorganic groups of PDMSUr matrix [13]. Observing the Figure 6A and 6B, the patterns of Silicon and Bromine correlate with their corresponding patterns of Tungsten, showing different atomic distributions due to the heterogeneous features that these materials exhibited during their elaboration. The presence of Bromine in these figures could due to its compound Tetraethylammonium Bromide (TEAB) that was assumed to be the catalyst o partial-catalyst in the previous step for synthesis of PDMSUr-PWA films [14]. Nonetheless, from these Bromine mappings one can infer the possibility that alternatively there are other species related of this chemical element. The presence of Bromine could be related with the corresponding adhesive, thermal-insulator, and anti-corrosive properties that these films exhibit. The Bromine quantification was reported in the [36].

3.2. Semi-Quantitative Analysis

They are shown the concentrations obtained by SR- μXRF for the hybrid materials detailed in the items 2.1.2.1-2.1.2.4. Tables 5-8 report the results of SR-μXRF analysis [8] for the hybrid films containing phosphotungstate described in Tables 1-4. The procedure steps in order to obtain the concentrations by SR- μXRF based on WinAxil 2.0 and PyMCA 4.4.0 programs [8], are depicted in the Figures 7 and 8.

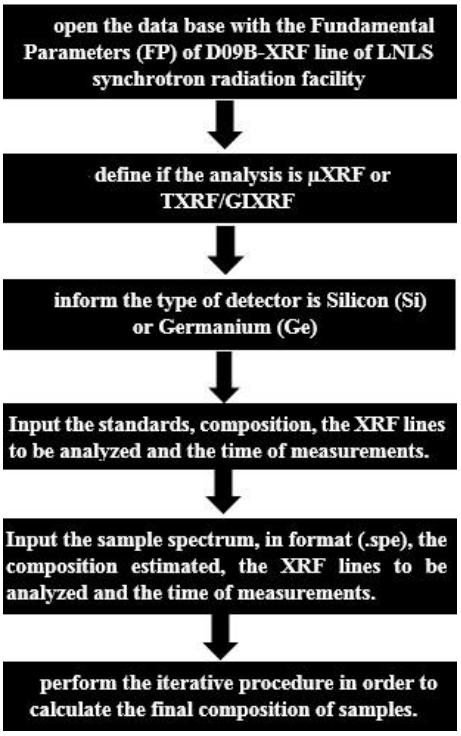

Figure 7*. Steps for semi-quantitative determination of the concentrations (%wt/wt) by WinAxil$_2$.0.*

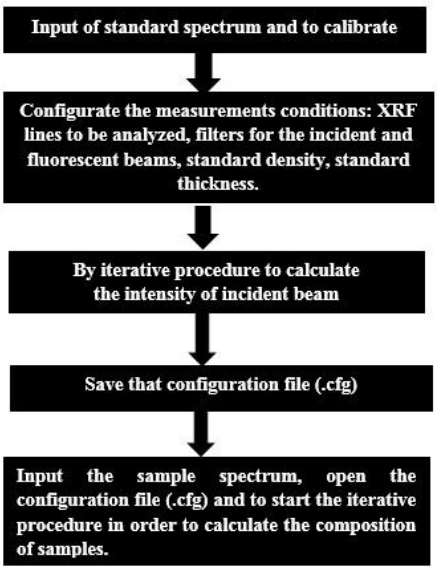

Figure 8*. Steps for semi-quantitative determination of the concentrations (%wt/wt) by PyMca 4.4.0.*

Table 5. *Titanium and Tungsten Concentrations obtained in the Hybrid ORMOSIL-TiO_2(NPs)- PWA films using WinAxil program [8].*

Code Sample	Titanium Concentration [Ti](%wt/wt)	SR-µXRF Coefficient of Variation [Ti](%wt/wt)	Tungsten Concentration [W](% wt/wt)	SR-µXRF Coefficient of Variation [W] (%wt/wt)
A7	0.81 ±0.09	11.1	55.1 ±0.2	0.4
A8	1.59 ±0.24	15.1	56.1 ±0.4	0.7

Table 6. *Zinc and Tungsten Concentrations obtained in the Hybrid ORMOSIL-Zn^{2+} ions-PWA films using PyMCA program [8].*

Code Sample	Zinc Concentration [Zn](%wt/wt)	SR-µXRF Coefficient of Variation [Zn](%wt/wt)	Tungsten Concentration [W](%wt/wt)	SR-µXRF Coefficient of Variation [W](%wt/wt)
Zn 0.5	0.19 ±0.02	10.5	54.8 ±2.8	5.1
Zn 1.0	0.41 ±0.02	4.9	56.9 ±2.4	4.2

Table 7. *Silicon and Tungsten Concentrations obtained in the Hybrid PI-ORMOSIL-PWA films by SR-µXRF using PyMCA program [8]. Reference method (ICP-OES).*

Sample	SR-µXRF Silicon Concentration [Si](%wt/wt)	SR-µXRF Coefficient of Variation [Si] (%)	ICP-OES Silicon Concentration [Si](%wt/wt)	SR-µXRF Tungsten Concentration [W](%wt/wt)	SR-µXRF Coefficient of Variation [W](%)	ICP-OES Tungsten Concentration [W](%wt/wt)
PATH-1	2.13 ±0.43	20.2	2.0 ±0.1	8.37 ±0.32	3.8	8.0 ±0.5
PATH-2	5.52 ±1.59	28.8	5.8 ±0.4	7.52 ±0.57	7.6	6.9 ±0.2
PATH-3	6.73 ±1.44	21.4	6.9 ±0.4	6.79 ±0.84	12.4	6.4 ±0.3

Table 8. *Tungsten Concentrations obtained in the Hybrid PDMSUr-PWA films by SR-μXRF using PyMCA program [8]. Reference method (NAA).*

Sample	SR-μXRF Tungsten Concentration [W](%wt/wt)	SR-μXRF Coefficient of Variation [W] (%)	NAA Tungsten Concentration [W](%wt/wt)	NAA Coefficient of Variation [W](%)
PUK-32	33.2 ±9.6	28.9	35.3 ±1.8	5.1
PUK-30	38.4 ±10.9	28.4	41.9 ±2.0	4.8
PUK-42	40.7 ±13.0	31.9	47.2 ±2.5	5.3

Comparing Table 5 with Table1, and Table 6 with Table 2, our results show a good agreement between the ratios of concentrations in sample preparation of ormosil films and those obtained by Fundamental Parameter Method (FP). From Tables 5-6 and Figure 3A-3B respectively, we can evidence that the intensity of W (signal) is increased; nonetheless the concentration of W undergoes only a little increase. Correlating Figure 5A-5C with the Coefficients of Variation in Table 7 for PI-ORMOSIL-PWA films", we can deduce that the Tungsten have a major homogeneity degree than Silicon (that exhibits values more than 20%) in its distribution [8]. The Coefficients of Variation for Tungsten in PDMSUr-PWA films (Table 8) at range [28-32%], which support this heterogenous distribution pattern illustrating in its SR-μXRF map (shown in Figure 6A).

From the comparison of Tungsten concentrations obtained using SR-μXRF (depth of analysis: hundreds of μm) and NAA (that there would not have limitations in its depth of analysis), whose results indicating homogeneity at bulk level (Coefficients of Variation≈5% in Table 8), we can see that with the increase of W nominal concentration (Table 4), there is segregation of this element within the thickness of PDMSUr-PWA films, which was reported by Elguera et al (2020) [22].

3.3. Estimation of Degree of Heterogeneity Obtained by SR-μXRF

Tables 9-15 show the estimative of degree of heterogeneity of Silicon, Titanium, Tungsten, Zinc obtained by SR-μXRF (for Tables 13-14, and 15 are considered ICP-OES and NAA results also) for the hybrid materials detailed in the items 2.1.2.1-2.1.2.4, using the information from Tables 5-8, by means of Horwitz Ratio (HorRat), according to the equations (1) and (2) in the page 4:

Table 9. *Estimative of HorRat's parameter for Titanium concentrations obtained by SR-μXRF for ORMOSIL-TiO_2(NPs)-PWA films (based on the Table 5).*

Sample's Code	$PRSD_R$	HorRat SR-μXRF	HorRat's Parameter expected value
A7	4.1	2.7	2.0
A8	3.7	4.0	2.0

Table 10. *Estimative of HorRat's parameter for Tungsten concentrations obtained by SR-μXRF for ORMOSIL-TiO_2(NPs)-PWA films (based on the Table 5).*

Sample's Code	$PRSD_R$	HorRat - SR-μXRF	HorRat's Parameter expected value
A7	2.2	0.3	2.0
A8	2.2	0.3	2.0

Table 11. *Estimative of HorRat's parameter for Zinc concentrations obtained by SR-μXRF for ORMOSIL-Zn^{2+}ions-PWA films [8] (based on the Table 6).*

Sample's Code	PRSDR	HorRat - SR- μXRF	HorRat's Parameter expected value
Zn 0.5	5.1	2.1	2.0
Zn 1.0	4.6	1.1	2.0

Table 12. *Estimative of HorRat's parameter for Tungsten concentrations obtained by SR-μXRF for ORMOSIL-Zn_2^+ions-PWA films [8] (based on the Table 6).*

Sample's Code	PRSDR	HorRat – SR- μXRF	HorRat's Parameter expected value
Zn 0.5	2.2	2.3	2.0
Zn 1.0	2.2	1.9	2.0

Table 13. *Estimative of HorRat's parameter for Silicon concentrations obtained by SR-μXRF and ICP-OES for PI-ORMOSIL-PWA films (based on the Table 7). [8].*

Sample's Code	PRSDR	HorRat – SR-μXRF	HorRat - ICP-OES	HorRat's Parameter expected value
PATH-1	3.6	5.7	1.4	2.0
PATH-2	3.1	9.3	2.2	2.0
PATH-3	3.0	7.1	1.9	2.0

Table 14. *Estimative of HorRat's parameter for Tungsten concentrations obtained by SR-μXRF and ICP-OES for PI-ORMOSIL-PWA films (based on the Table 7). [8].*

Sample's Code	PRSDR	HorRat - SR-μXRF	HorRat - ICP-OES	HorRat's Parameter expected value
PATH-1	2.9	1.3	2.1	2.0
PATH-2	3.0	2.6	1.0	2.0
PATH-3	3.0	4.1	1.5	2.0

Table 15. *Estimative of HorRat's parameter for Tungsten concentrations obtained by SR-μXRF and NAA for PDMSUr-PWA films (based on the Table 8). [8].*

Sample's Code	PRSDR	HorRat - SR-μXRF	HorRat- NAA /	HorRat's Parameter expected value
PUK-32	2.3	12.2	2.2	2.0
PUK-30	2.3	12.3	2.1	2.0
PUK-42	2.2	13.9	2.4	2.0

4. Discussion

4.1. For ORMOSIL-TiO_2(NPs)-PWA Films

The estimation of HorRat parameter for Titanium (Ti) concentrations obtained by SR- μXRF (Table 9) exhibits values higher than the expected value (2.0), indicating heterogeneity in the distribution of this chemical element, which is agree with Table 5 (Coefficients of Variation >10%). This non-homogeneity of Titanium can affect the performance of optical properties of ormosil films. On another hand, for Tungsten (W) concentrations (Table 10), the HorRat parameters are less than 2.0, which indicate homogeneity in its distribution. These results are agreed with Table 5 (Coefficients of Variation < 5%) and with the SEM-EDX maps of Tungsten (W) of these materials ([6]), whose show its homogeneous atomic-distribution at surface level and at depth level up to 1 μm [6].

4.2. For ORMOSIL-Zn^{2+}ions-PWA Films

The estimation of HorRat parameter for Zinc concentrations obtained by SR-μXRF (Tables 11) exhibits values less and closer than the expected value (2.0), indicating homogeneity in their atomic-distribution. The estimation of HorRat parameter for Tungsten concentrations obtained by SR-μXRF (Table 12) exhibits values closer than to the expected value (2.0), indicating homogeneity in this distribution. These homogenous distributions are in concordance with the STEM characterization reported by Ferreira Neto et al (2014) that shows small aggregates (polydispersity range: 30- 500 nm), which are uniformly scattered in a homogenous matrix ([6]). In addition, Nano-EDX analysis revealed that those aggregates are constituted by Tungsten (probably as phosphotungstic acid- PWA) and Zn [10].

4.3. For PI-ORMOSIL-PWA Films

The estimation of HorRat parameter for Silicon concentrations obtained by SR-μXRF (Table 13) exhibits values higher than the expected value (2.0), indicating heterogeneity in its atomic-distribution. The estimation of HorRat parameter for Tungsten concentrations obtained by SR-μXRF (Table 14) exhibits values higher than the expected value (2.0), except for PATH-1 sample, indicating non-homogeneity in its distribution. This exception may have been related with was reported by Ferreira et al (2016) about that with the increase of PWA concentration lead to more homogeneous PI-ORMOSIL-PWA films [12]. For Silicon and Tungsten concentrations obtained by ICP-OES (Tables 13 and 14), the HorRat parameters obtained exhibits values less and closer than the expected value (2.0). This homogeneity for the ICP-OES results can due to that this method of analysis consist in the total destruction of sample, minimizing the possible molecular interferences. Thus, these results could be used as reference, due to the no existence of standards for PI-ORMOSIL-PWA films.

4.4. For PDMSUr-PWA Films

The estimation of HorRat parameter for Tungsten concentrations obtained by SR- μXRF (Table 15) exhibits values far than the expected value (2.0), indicating heterogeneity in the distribution of this chemical element, which is agree with Table 8 (Coefficients of Variation >25%). On another hand, for Tungsten concentrations obtained by NAA (Table 15), the HorRat parameters obtained are around 2.0. Thus, these results could be used as reference for PDMSUr-PWA films, because for this method of analysis in theory the depth of the sample does not constitute an obstacle. The knowledge of heterogeneity of Tungsten distribution is necessary in order to correlate their mechanical properties (elastic modulus and hardness) that these films exhibit [8].

5. Conclusions

In the present investigation, we show the study based on Synchrotron Radiation X-ray Microfluorescence (SR-μXRF) of materials at micrometric and nanometric scales. These materials were prepared based on Sol-Gel Chemistry, which is used for low-temperature synthesis of ceramics, nanocomposites and hybrid (inorganic/organic) materials. For this case, we work with Ormosil (Organically Modified Silicates), which belongs to the Class II of hybrid materials having potential uses as optical materials, chemical sensors, catalysts, membranes, self-cleaning coatings. SR-μXRF was used in order to determine the local concentration, as far the correlation between elements and their localization. We have presented data demonstrating the application of SR-μXRF as semi-quantitative determination method at local level of these hybrid materials, which is very useful due to the non-existence of certified standards. The approximated estimation of HorRat parameters has revealed that concentrations obtained by ICP-OES and NAA can be used as reference values for comparison with the corresponding SR-μXRF results, in order to have hints about segregation at surface and at bulk level. About the concern of the estimation of degree of heterogeneity obtained by SR-μXRF:

1. For Hybrid ORMOSIL-TiO_2(NPs)-PWA films, SR-μXRF is a useful analytical tool for qualitative determination of Titanium (Ti), which is heterogeneously distributed and spatially it is proximate (sometimes as isolated-regions) to the Tungsten (W) regions. From SR-μXRF mappings (depth of analysis: tens of μm) and EDX maps (depth of analysis: up to 1 μm) of Tungsten it can be inferred that in these films this element is homogeneously distributed at micrometric level.
2. For Hybrid ORMOSIL-Zn^{2+}ions-PWA films the Zinc (Zn) and Tungsten (W) are homogeneously distributed and practically share spatially the same region.
3. For PI-ORMOSIL-PWA films, SR-μXRF mapping have shown the non- homogenous distribution of the Silicon (Si) and quasi-homogenous distribution of Tungsten (W). SR-μXRF concentrations for Silicon (Si) and Tungsten (W) are convergent with the corresponding results obtained by ICP-OES.
4. For PDMSUr-PWA films, SR-μXRF mapping have shown the heterogenous distribution pattern for Tungsten (W), as also the capacity for identification of Bromine (Br) in these materials.

HorRat parameters for concentrations obtained by ICP-OES and NAA (bulk analyses) are close to the expected value (2.0), which make possible using as reference values for SR-μXRF results due to the non-existence of standards of these hybrid materials. SR- μXRF mappings gives indications about a direct relation among the intensities of Titanium (Ti) and Zinc (Zn) with the increase of the Tungsten (W) intensity. From SR- μXRF correlation spatial mapping and previous

Raman/IR/XANES/FTMIR/ATR analysis, we can infer electrostatic/intermolecular interactions among polyoxometalates ($[PW_{12}O_{40}]^{3-}$/PWA) and the other chemical groups, constituents of these four different types of Hybrid films. SR-μXRF has demonstrated to be the appropriate method of analysis for these hybrid films.

Abbreviations

Ormosil	Organically Modified Silicates
HorRat	Horwitz Ratio
SR-μXRF	Synchrotron Radiation X-ray Microfluorescence

Acknowledgments

The author thanks to the São Paulo Research Foundation (FAPESP) by the research grants (2011/08120-0, 2011/06019-0 and 2013/05279-3) and to the CNPq Brazilian agency by the financial support (research grants 141880/2011-2 and 160515/2011-4). We also extend our gratitude to the Dr. Carlos Perez for his help at the SR-μXRF measurements done (2011-2015) at Brazilian Synchrotron Light Source (LNLS) and for his help with the experimental setup picture, to the CNPEM-LNLS facilities for SR-μXRF measurements (proposal number: XAFS1 14257), to Dr. Cibele Zamboni for the NAA measurements performed (2014-2015) at Nuclear and Energetic Research Institute-São Paulo-Brazil (IPEN/CNEN- SP). Finally, the author thanks to Dr. Prof. Wagner Polito of the Institute of Chemistry of São Carlos, University of São Paulo, São Carlos-SP-Brazil (IQSC-USP) for his advices and discussions about of the Methodology of Analysis (based on Standardless condition and Test of Homogeneity); and to the Inorganic Hybrid Materials Chemistry Group (GQMATHI-IQSC-USP).

Author Contributions

Orlando Elguera Ysnaga is the sole author. The author read and approved the final manuscript.

Conflicts of Interest

The author declares no conflicts of interest.

References

[1] F. Hutter, K., Haas, H. Schmidt. "Ormosiles-A New Class of Materials for Sensitive Layers in the Development of Gas Sensors". Proc. of the 2nd International Meeting on Chemical Sensors, Bordeaux. 1986: 4-15. http://dx.doi.org/10.22028/D291-24325

[2] J. Mackenzie, E. Bescher. "Structures, Properties and Potential Applications of Ormosil". Journal of Sol-Gel Science and Technology. 1998. 13: 371-377. https://doi.org/10.1023/A:1008600723220

[3] J. D. Wright, N. A. J. M. Sommerdijk. (2000). Sol-Gel Materials: Chemistry and Applications (1st ed.). Advanced Chemistry Texts. (Inglés). CRC Press. https://doi.org/10.1201/9781315273808

[4] J. David, P. Smith, J. Hay, J. Watts. "The Effect of Ormosil Nano-Particles on the Toughness of a Polyester Resin". Journal of Materials Science. 2007. 43: 3230-3237. https://doi.org/10.1007/s10853-006-0231-4

[5] V. Tripathi, V. Kandimalla, J. Huangxian. "Preparation of ormosil and its applications in the immobilizing biomolecules". Sensors and Actuators B. 2006. 114(2): 1071– 1082. https://doi.org/10.1016/j.snb.2005.07.037

[6] L. P. Gonçalves. Nanopartículas de Titânio como aditivos em materiais híbridos inorgânicos fotocrômicos baseados em fosfotungstatos. [Master of Science in Materials Engineering Dissertation]. São Carlos, São Paulo-Brasil: Instituto de Química de São Carlos/ Escola de Engenharia de São Carlos, Universidade de São Paulo (EESC-USP/IQSC-USP), 2011.

[7] L. Gonçalves, E. Ferreira-Neto, S. Ullah, et al. "Enhanced Photochromic Response of Ormosil–Phosphotungstate Nanocomposite Coatings Doped with TiO_2 Nanoparticles". J. Sol-Gel Sci. Technol. 2015. 76(2): 386–394. https://doi.org/10.1007/s10971-015-3787-0

[8] O. A. Elguera Ysnaga. Métodos de Análise de Materiais Híbridos: Um estudo comparativo entre Fluorescência de Raios-X com Detecção Dispersiva em Energia usando Fonte Tradicional e Luz Síncrotron. [Doctor of Science in Analytical and Inorganic Chemistry, Thesis]. São Carlos, São Paulo-Brasil: Instituto de Química de São Carlos, Universidade de São Paulo (IQSC-USP), 2015. Pp. 249–301.

[9] E. Paiva Ferreira Neto. Preparação, Caracterização e Comportamento Fotocrômico de Filmes Híbridos de Ormosil-Fosfotungstato dopados com Nanopartículas de ZnO. [Completion Course Job's - CCJ]. São Carlos, São Paulo-Brasil: Instituto de Química de São Carlos, Universidade de São Paulo (IQSC-USP), 2011.

[10] E. Ferreira-Neto, S. Ullah, O. Elguera Ysnaga, U. P. Rodrigues-Filho. "Zn^{2+} doped Ormosil–Phosphotungstate Hybrid Films with Enhanced Photochromic Response". J. Sol-Gel Sci. Technol. 2014. 72(2): 290–300. https://doi.org/10.1007/s10971-014-3404-7

[11] F. Ferreira. Desenvolvimento de Materiais Híbridos baseados em Poliimida. [Doctoral Thesis in Materials Engineering]. São Carlos, São Paulo-Brasil: Escola de Engenharia de São Carlos, Universidade de São Paulo (EESC-USP), 2014.

[12] F. Ferreira, T. Amaral, O. Elguera Ysnaga, M. A. Pereira-Da-Silva, J. H. Lopes, J. P. Lewicki, M. A. Worsley, J. F. Schneider, G. Tremiliosi-Filho, U. P. Rodrigues-Filho. "Structure–Property Relationship of New Polymide–Organically Modified Silicate– Phosphotungstic Acid Hybrid Material System". J. Mater. Sci. 2016. 51: 4815–4824. https://doi.org/10.1007/s10853-016-9773-2

[13] K. Rossi Flores de Aguiar. S íntese de hidroxiuretana-poli (dimetilsiloxano) com diferentes termina ções de cadeia via fixa ção de CO_2: s íntese, caracteriza ções eaplica ções. [Doctor of Science in Analytical and Inorganic Chemistry, Thesis]. S ão Paulo-Brasil: Instituto de Qu ímica de S ão Carlos, Universidade de S ão Paulo (IQSC- USP), 2015.

[14] K. R. Aguiar, V. G. Santos, M. Eberlin, et al. ‘‘Efficient Greensynthesis of Bis (Cyclic Carbonate) Poly (Dimethylsiloxane) Derivative Using CO_2 Addition: A Novel Precursor for Synthesis of Urethanes’’. RSC Adv. 2014. 4(46): 24334–24343. https://doi.org/10.1039/C4RA03846K

[15] K. M. F. Rossi de Aguiar, E. P. Ferreira-Neto, S. Blunk, J. F. Schneider, C. A. Picon, C. M. Lepienski, K. Rischka and U. P. Rodrigues-Filho. ‘‘Hybrid Urethanesil Coatings for Inorganic Surfaces Produced by Isocyanate-Free and Sol-Gel Routes: Synthesis and Characterization’’. RSC Adv. 2016. 6(23): 19160–19172. https://doi.org/10.1039/C5RA24331A

[16] K. Tsuji. “Micro-X-ray Fluorescence”. Encyclopedia of Analytical Chemistry, online 2010. https://doi.org/10.1002/9780470027318.a9067

[17] F. Adams, K. Janssens, A. Snigirev. “Microscopic X-ray fluorescence analysis and related methods with laboratory and synchrotron radiation sources”. Journal of Analytical Atomic Spectrometry. 1998. 13: 319–331. https://doi.org/10.1039/A707100K

[18] K. Janssens, W. De Nolf, G. Van der Snickt, L. Vincze, B. Vekemans, R. Terzano, F. Brenker. “Recent trends in quantitative aspects of Microscopic X-ray fluorescence analysis”. TrAC Trends in Analytical Chemistry. 2010. 29(6): 464-478. https://doi.org/10.1016/j.trac.2010.03.003

[19] S. Smolek, C. Streli, N. Zoeger, P. Wobrauschek. “Improved Micro X-ray Fluorescence Spectrometer for light element analysis”. The Review of Scientific Instruments. 2010. 81(5): 053707. https://doi.org/10.1063/1.3428739

[20] T. Nakazawa, K. Nakano, K. Tsuji. “Development of a high - resolution confocal Micro-XRF instrument equipped with a vacuum chamber”. X-ray Spectrometry. 2013. 42(5): 374-379. https://doi.org/10.1002/xrs.2458

[21] K. Janssens, F. Adams, A. Rindbly. Microscopic X-ray Fluorescence Analysis. Chichester, UK: John Wiley and Sons, Ltd., 2000.

[22] X. Ding, Y. He, Y. Yan. ‘‘X-ray source for X-ray Microfluorescence using a Monolithic X-ray Focusing Lens Combined with Aperture Optics’’. X-ray Spectrometry. 1997. 26: 374-379. https://doi.org/10.1002/(SICI)1097-4539(199711/12)26:6<374::AID-XRS236>3.0.CO;2-S

[23] A. Iida. ‘‘X-ray Spectrometric Applications of a Synchrotron X-ray Microbeam’’. X- ray Spectrometry. 1997. 26(6): 359-363. https://doi.org/10.1002/(SICI)1097-4539(199711/12)26:6<359::AID-XRS234>3.0.CO;2-L

[24] K. Janssens, L. Vincze, A. Aerts, et al. ‘‘Synchrotron Radiation Induced X-ray Microfluorescence Analysis’’. Mikrochim. Acta Suppl. 1996. 13: 87–115. https://doi.org/10.1007/978-3-7091-6555-3_5

[25] M. Rauwolf, A. Turyanskaya, A. Roschger, J. Prost, R. Simon, O. Scharf, M. Radtke, T. Schoonjans, A. Buzanich, K. Klaushofer, P. Wobrauschek, J. Hofstaetter, P. Roschger, C. Streli. ‘‘Synchrotron radiation Micro X-ray fluorescence spectroscopy of thin structures in bone samples: comparison of confocal and color X-ray camera setups’’. Journal of Synchrotron Radiation. 2017. 24: 307-311. https://doi.org/10.1107/S1600577516017057

[26] J. Sherman. ‘‘The Theoretical Derivation of fluorescent X-ray intensities from mixtures’’. Spectrochimica Acta. 1955. 7: 283-306. https://doi.org/10.1016/0371-1951(55)80041-0

[27] C. Rivera, R. Rodr guez. ‘‘Horwitz Equation as Quality Benchmark in ISO/IEC 17025 Testing Laboratory’’. Published in www.bii.mx 2014.

[28] W. Horwitz, R. Albert. ‘‘The Horwitz Ratio (HorRat): A Useful Index of Method Performance with Respect to Precision’’. Journal of AOAC INTERNATIONAL (J AOAC Int.). 2019. 89(4): 1095–1109.

[29] T. Wolff, W. Malzer, I. Mantouvalou, O. Hahn, B. Kanngie ßer. ‘‘A new fundamental parameter-based calibration procedure for Micro X-ray fluorescence spectrometers’’. Spectrochim. Acta, Part B. 2011. 66: 170-178. https://doi.org/10.1016/j.sab.2011.01.009

[30] C. P érez, M. Radtke, H. S ánchez, H. Tolentino, R. Neuenshwander, W. Barg, M. Rubio, M. Silveira Bueno, I. Raimundo, J. Rohwedder. ‘‘Synchrotron Radiation X-ray Fluorescence at the LNLS: Beamline Instrumentation and Experiments’’. X-Ray Spectrometry. 1999. 28(5): 320–326. https://doi.org/10.1002/(SICI)1097-4539(199909/10)28:5<320::AID-XRS359>3.0.CO;2-1

[31] PyMca Home. 2015. http://pymca.sourceforge.net/documentation.html [accessed April 3 2015].

[32] V. Sol é, E. Papillon, M. Cotte, Ph. Walter, J. Susini. ‘‘A Multiplatform Code for the Analysis of Energy-Dispersive X-ray Fluorescence Spectra’’. Spectrochim. Acta, Part B. 1999. 62(1): 63–68. https://doi.org/10.1016/j.sab.2006.12.002

[33] P. Van Espen, K. Janssens, I. Swenters. Manual for AXIL Software. Canberra-Packard: Antwerp, 1994.

[34] Canberra Eurisys Benelux N. V. WinAxil Brief Operational Guide. Manual version 2.0 March 2006.

[35] P. Gouffon. (1987). Manual do programa IDEFIX. Instituto de F ísica da Universidade de S ão Paulo (IFUSP), S ão Paulo, Brazil.

[36] Orlando Elguera Ysnaga (2020) “Qualitative and Semiquantitative Determination of Bromine in Hybrid Hydroxyurethanes-Poly (dimethylsiloxane) Films Containing Phosphotungstates ($[PW_{12}O_{40}]^{3-}$)” Engineering Physics 4(2): 19-36. https://doi.org/10.11648/j.ep.20200402.11

[37] O. Elguera, K. Rossi de Aguiar, C. Zamboni, W. Polito, U. P. Rodrigues-Filho (2020) "Qualitative and Semiquantitative Determination of the Atomic and Molecular Tungsten Distributions in Hybrid Hydroxyurethanes- Poly (dimethylsiloxane) Films Containing Phosphotungstates ($[PW_{12}O_{40}]^{3-}$)". Applied Spectroscopy. 74(12): 1515-1529.
https://doi.org/10.1177/0003702820945018

Research Fields

Orlando Elguera Ysnaga: Micro-XRF, TXRF/GIXRF., Synchrotron, Ormosil Analysis, Semiquantitative analysis, Bi-dimensional Elementary Mapping, ICP-OES